THE JOURNAL OF PHYSICAL CHEMISTRY B

Article

pubs.acs.org/JPCB

# Liquid Dimethyl Carbonate: A Quantum Chemical and Molecular Dynamics Study

Sandeep K. Reddy and Sundaram Balasubramanian*

Chemistry and Physics of Materials Unit, Jawaharlal Nehru Centre for Advanced Scientific Research, Jakkur, Bangalore 560 064, India

Supporting Information

**ABSTRACT:** A density functional theory based Car−Parrinello molecular dynamics simulation of liquid dimethyl carbonate, an environmentally benign solvent, has been carried out to study its structure and dynamics. Conformational excitations of the molecule have been probed in both its gas and liquid phases. While the cis−cis conformer is the global energy minimum and, thus, the most predominant, at ambient conditions a few percent of molecules are present in the cis−trans conformation as well. The latter possesses a dipole moment of around 4.5 D in the liquid state, a value that is nearly five times as large as that for the cis−cis conformer. Dipole−dipole interactions play a crucial role in the formation of small hydrogen bonded clusters of cis−trans conformers in the liquid. The vibrational spectrum of liquid dimethyl carbonate has been obtained from the trajectory and is shown to agree quite well with available experimental data.

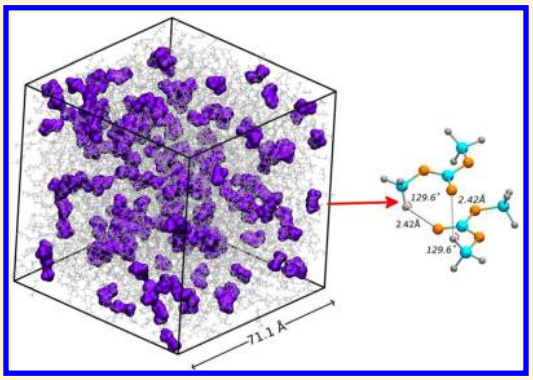


## 1. INTRODUCTION

Green chemical processes have attracted much attention in recent years due to environmental concerns and to increase efficiency. The concept was formally introduced in 1991 by Anastas, aimed at carrying out syntheses to reduce or eliminate hazardous substances.[1] Some of the characteristics of green syntheses include avoiding the use of toxic compounds, promoting the use of biodegradable, renewable, and less volatile substances, reducing energy needs, and adoption of routes that yield no hazardous byproducts. It is important to use environmentally friendly solvents in many chemical reactions without decreasing their yield or rate. Dimethyl carbonate (DMC), an organic liquid containing both polar and nonpolar groups is one such. It belongs to the family of carbonate esters and has been used as a solvent for several chemical reactions over many decades. It is almost immiscible in water, but soluble in many organic solvents such as diethyl ether, methanol, and so on. It has been used as a solvent for electrochemical and extractive applications. In recent years, researchers have promoted the use of dimethyl carbonate as a viable, green solvent due to its low volatility, nonflammability, nontoxicity, and biodegradability.[2,3] It is used in methylation and carbonylation reactions to substitute for harmful, toxic, and corrosive solvents such as dimethyl sulfate, methyl halides, and phosgene and to conduct chemical reactions in environmentally safety media.[3,4] It has found applications in the fuel industry due to its high oxygen weighting (53%), higher than the normally used additive solvent, tert-butyl methyl ether.[5] It is regarded as a good additive to gasoline to reduce carbon monoxide in auto exhaust.[6−8] DMC is used in lithium batteries to dissolve lithium ions due to its low volatility, long shelf life, increased battery power density and an overall reduction in manufacturing costs.[9] Very recently, it was shown that DMC can be used in completely controlled stereo- and regioselective ring-opening chemical reactions in an eco friendly, green condition by replacing toxic solvents, dichloromethane, diethyl ether, acetonitrile, and acetone.[3] Although the Suzuki−Miyaura coupling reaction was reported to have been carried out in DMC without any metal, a recent report has found trace amounts of metal that could have catalyzed the reaction.[10,11]

Knowing the importance of this liquid in green and environmental chemistry, many attempts have been made to explore its structure both experimentally and theoretically. Spectroscopic studies were carried out to explore the conformational stability of the molecule in gas and liquid phases. They showed that cis−cis conformers are the dominant species among all possible conformers, namely, cis−cis, cis−trans, and near-trans−near-trans.[12,13] Based on IR absorbance data, the enthalpy difference between the cis−cis and cis−trans conformers has been estimated to be 2.60 ± 0.5 kcal/mol.[12] Dielectric studies on liquid DMC at room temperature have discovered the presence of a high dipole moment conformer, the near-trans−near-trans one.[14] Its gas-phase structure has been determined using electron diffraction.[15] The earliest empirical potential based molecular dynamics simulations of the liquid at 80 °C was reported in 1998 and around 68% of molecules were reported to be in the cis−cis conformation at this temperature, which deviates from the value estimated from Boltzmann distribution.[16] Soetens et al. have carried out molecular dynamics simulations using the OPLS and CFF91

Received: September 21, 2012
Revised: November 28, 2012
Published: December 2, 2012





dx.doi.org/10.1021/jp309374m | J. Phys. Chem. B 2012, 116, 14892−14902

derived force field on liquid DMC and their interest was limited to the structure and analyzed using pair correlations functions (PCF).[17] Recently, Gontrani et al. have reported the first X-ray diffraction data of liquid DMC. The structure of the liquid was analyzed by calculating structure factors and PCFs and by comparing against OPLS force field based molecular dynamics simulations.[18,19]

Here, we report a Car−Parrinello molecular dynamics (CPMD) study of liquid DMC. The density functional theory protocols are benchmarked against MP2 level quantum chemical calculations for the molecules in gas phase. Liquid state structure is investigated using pair correlation functions and spatial density maps. Conformational equilibrium is compared against both experimental and force field based simulations. This paper is divided into four sections. The next section details the computational techniques and is followed by results on structure and dynamics analyzed using tools such as pair correlation functions, spatial distribution functions, dipole−dipole correlations, and vibrational power spectrum. The last section summarizes the results.

## 2. COMPUTATIONAL DETAILS

Three sets of calculations were carried out on dimethyl carbonate. First, gas phase calculations have been performed to obtain the stability and dipole moments of its conformers. Second, classical molecular dynamics simulations were performed to obtain initial configurations for CPMD simulations and also to compare against the CPMD results. Third, using these final geometries, a Car−Parrinello molecular dynamics simulation trajectory of liquid DMC under ambient conditions was generated. In addition, to understand the spatial distribution of molecules with specific conformations, a classical MD simulation of a very large system was also carried out.

The gas phase calculations were performed using the Gaussian09 package[20] for which initial structures were constructed using GaussView.[20] The potential energy of a single molecule was also calculated at MP2/aug-cc-pvdz level of theory as a function of the two dihedrals. Harmonic frequency calculations were also performed at the same level of theory to locate any imaginary modes.

A system consisting of 96 molecules was generated by placing DMC molecules in a cubic box of length 100 Å. Initial coordinates were generated by replicating coordinates of single molecule in three dimensions such that the distance between neighboring molecules was 9 Å. Three dimensional periodic boundary conditions on a cubic simulation cell were employed. This system was equilibrated in the isothermal−isobaric ensemble (NPT) for 1 ns. The force field was the same as used by Caminiti et al., which belongs to the OPLS framework.[18,19] Temperature (293 K) and pressure (1 atm) controls were achieved using Nóse-Hoover thermostat and barostat, respectively, with relaxation times of 1 ps each. Nonbonded interactions were calculated using 12-6 Lennard-Jones and Coulombic potentials within a spherical cutoff of 11.5 Å. The long-range part of the electrostatic interaction was calculated using the particle−particle particle mesh (PPPM) solver with a precision of $10^{-5}$. All the C−H bonds were constrained to equilibrium values using the SHAKE algorithm. A time step of 1 fs was used. The average density of the simulated system was found to be 1.076 g/cm$^3$, very close to the experimental value of 1.0687 g/cm$^3$, resulting in a mean box length of 23.717 Å. The final coordinates of this run were scaled with the mean box length. This set was used as the initial coordinates for a constant NVT MD trajectory for a duration of 10 ns. The final coordinates from this run was used as a starting configuration for the Car−Parrinello molecular dynamics simulation. Classical MD simulations were carried out using LAMMPS.[21]

CPMD simulations were carried out using the CPMD-3.13.2 package.[22] A fictitious electron mass of 400 au and a time step of 4 au were employed. This combination has earlier been employed successfully by others to produce stable trajectories.[23,24] In our CPMD simulation, the fictitious electron kinetic energy exhibited no drift in time, implying the adiabatic separation between nuclear and electronic degrees of freedom. The ion temperature was maintained at 293 K using the Nóse-Hoover chain thermostat.[25] As mentioned before, the system contained 96 DMC molecules (i.e., 1152 atoms) in a cubic box of edge length 23.7 Å. The wave function of the valence electrons were expanded in a plane wave basis set with an energy cutoff of 85 Ry and a density cutoff of 340 Ry. The effect of all the core electrons and of the nucleus on these valence electrons was considered by using norm conserving Troullier-Martins pseudopotentials.[26] The total number of valence electrons was 3456. The Perdew, Burke, and Enzerhof (PBE) exchange-correlation functional was employed.[27] The effect of van der Waals interactions (vdW) was considered through empirically determined dispersive interaction terms, the parameters of which were taken from Williams and Malhotra.[28] Such calculations henceforth will be referred to as PBE+vdW in the rest of this manuscript. Note that some of these parameters were validated by us in an earlier CPMD simulation study of supercritical carbon dioxide.[29] All hydrogens were replaced by deuterium so as to be able to treat the dynamics classically. The system was equilibrated for 3 ps followed by the generation of an analysis trajectory of 10 ps. Coordinates were dumped at every time step. Unless specified, pair correlation functions were calculated using a bin width of 0.1 Å.

The trajectory in CPMD simulations is likely to explore only local structural rearrangements in the liquid, relative to the initial configuration generated from the initial FFMD simulation. We have observed a significant relaxation of the first coordination shell of a given molecule, even within 1 ps of initiating the CPMD run. In Figure S1 of Supporting Information, we compare the pair correlation function between atom types O and HC, obtained over several time windows in the CPMD run and that obtained from the FFMD simulation. The formation of an intermolecular hydrogen bond can be examined through this specific pair correlation function. We note the significant change in this function calculated within 1 ps of the initiation of the CPMD run, relative to that obtained from FFMD. The functions calculated beyond 2−3 ps of starting the CPMD trajectory are stationary. We thus believe that the CPMD run length, however short, is sufficient to probe the first neighbor structural relaxations on the PBE+vdW surface.

Dipole moments were calculated using maximally localized Wannier functions (MLWFs).[30] The dipole moments of individual molecules were calculated using the formula

$$\mu_i = \sum_i e_i \times R(i) - 2\sum_j W(j) \quad (1)$$

where $R(i)$ and $e_i$ are the position and valency of atom $i$, respectively, and $W(j)$ is the position of Wannier center. A total of 20 equally spaced configurations from the analysis trajectory

were selected for the calculation of the molecular dipole moments. Vibrational density of states in the liquid was calculated by taking the Fourier transform of velocity autocorrelation function.

The systems were visualized using Gaussview,[20] Jmol,[31,32] and VMD.[33]

## 3. RESULTS AND DISCUSSION

**Gas-Phase Calculations.** *Monomers.* The molecular geometry of DMC and atom indices are shown in Figure 1.

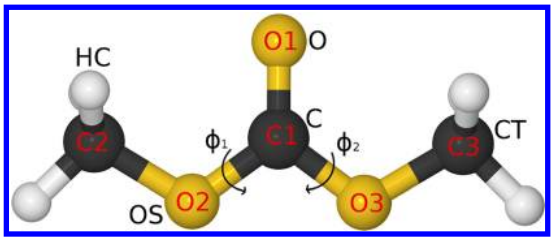


**Figure 1.** cis−cis Conformer of dimethyl carbonate.

Initial geometries of DMC were obtained by fixing the values of the two dihedrals $\phi_1$ and $\phi_2$, either at 0° or 180°, and varying the other. Geometry optimization was carried out at fixed dihedral angle values at MP2 level of theory with different basis sets. Here, $\phi_1$ is the torsional angle formed by the two planes, O1−C1−O2 and C1−O2−C2, while $\phi_2$ is that formed by O1−C1−O3 and C1−O3−C3 planes. Three stable conformers are located on the potential energy surface. These are cis−cis, cis−trans, and trans−(near-trans). Their geometries and an additional conformer are displayed in Figure 2. The energy

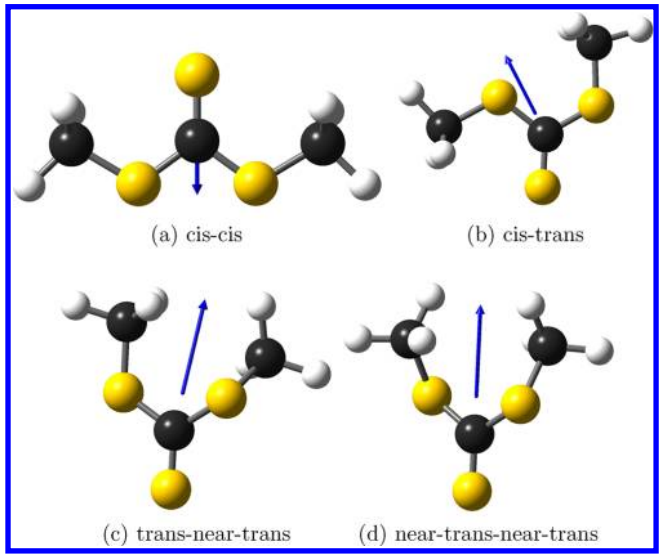


**Figure 2.** Conformers of dimethyl carbonate. Dipole moment vector is shown in blue color. Color code: C, black; O, yellow; H, white.

profile as a function of the torsional angles is shown in Figure 3. In the trans−(near-trans) conformer ($\phi_1$ = 180°, $\phi_2$ = 115°), one methyl group is present in the plane of the molecule, while the other methyl group is away from the plane. The cis−cis conformer in which both the dihedral angles are zero is the most stable. Compared to this conformer, the cis−trans and the trans−(near-trans) conformers are higher in energy by 3.17 and 17.29 kcal/mol, respectively. The relative energy of the cis−

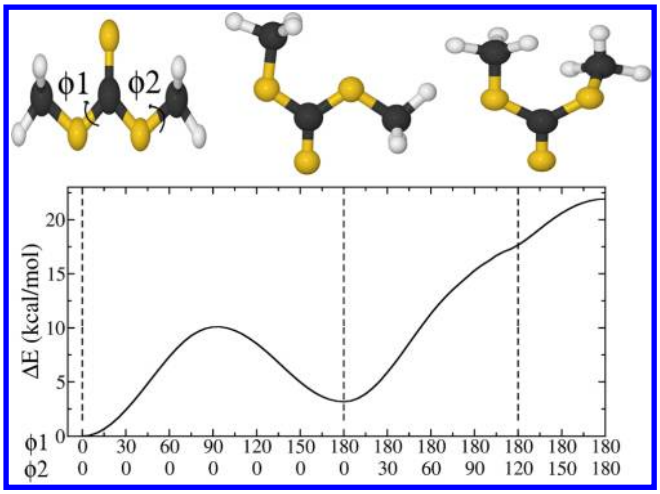


**Figure 3.** Energy profile of dimethyl carbonate (bottom) as a function of two dihedral angles, $\phi_1$ and $\phi_2$ calculated at MP2/aug-cc-pVDZ level of theory. The vertical dotted lines show the positions of the three minima. Corresponding structures are also shown (top).

trans conformer with respect to the most stable conformer, that is, cis−cis, calculated through different methods is shown in Table 1. The energy barrier between the cis−cis and cis−trans

**Table 1. Energy (kcal/mol) of cis−trans Conformer Compared to cis−cis Conformer Calculated at Different Levels of Theory**

| method | energy difference (kcal/mol) |
|---|---|
| HF/6-31(d) | 3.75 |
| B3LYP/6-311(2d,d,p) | 2.90 |
| MP2/6-311(2d,d,p) | 3.50 |
| MP2/aug-cc-pVDZ | 3.21 |
| MP2/aug-cc-pVQZ | 3.17 |
| OPLS | 2.58 |
| PBE/PW | 2.72 |
| PBE+vdW/PW | 2.46 |

conformer is 10.10 kcal/mol. The local stabilization of the trans−(near-trans) conformer arises from the electrostatic interaction between the hydrogen atom of the methyl group and the carbonyl oxygen.

The rather large energy difference between the cis−cis and the cis−trans conformers makes the latter quite unfavorable. Occurrence of the trans−(near-trans) conformer is even less likely. To search for any other stable conformer of DMC, a 2D potential energy surface was generated by performing geometry optimization of modeled structures. These structures were obtained by varying the two dihedrals, $\phi_1$ and $\phi_2$ in steps of 10° each. In this manner, a total of 360 geometries were obtained and all of them were optimized by constraining the values of the two dihedrals. Figure 4 shows the 2D potential energy surface. In addition to the above three minima, a new minimum is found corresponding to the dihedrals, $\phi_1$ = 140.8° and $\phi_2$ = 140.8°. The position of this new minimum is shown by an arrow in Figure 4 and is named as (near-trans)−(near-trans) conformer. It is higher in energy by 16.06 kcal/mol compared to the cis−cis conformer, but is more stable than the trans−(near-trans) conformer by 1.23 kcal/mol. Hessian-based harmonic frequency calculations of all the above conformers exhibit no imaginary frequency confirming that these are


dx.doi.org/10.1021/jp309374m | J. Phys. Chem. B 2012, 116, 14892−14902

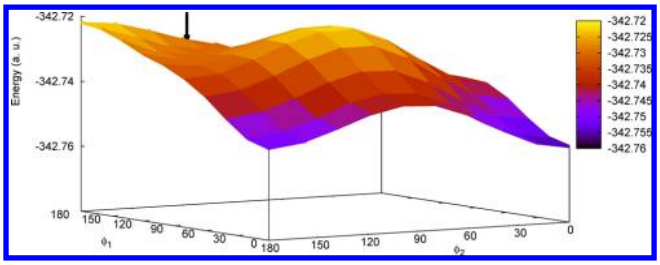


**Figure 4.** Potential energy of dimethyl carbonate as a function of two dihedrals, $\phi_1$ and $\phi_2$. The position of the near-trans−near-trans minimum is indicated by an arrow.

minima on the potential energy surface. Frequency calculation on the trans−trans conformer ($\phi_1$ = 180°, $\phi_2$ = 180°) shows one imaginary frequency indicating that it is unstable.

Knowledge of the dipole moment of different conformers of DMC can help us to better understand the intermolecular structure in the liquid state. Experimental values for the dipole moments of cis−cis and cis−trans conformers in the gas phase have been reported.[14,34−36] However, quantitative agreement between values reported by several authors is rather poor. Values reported for the cis−cis conformer are in the range of 0.3−0.8 D and for the cis−trans conformer, they are between 1.7 and 3.1 D.[14,34−36] We have calculated the dipole moment values of all these conformers in gas phase at MP2/aug-cc-pVDZ level of theory. The calculated values are 0.32, 3.98, 5.78, and 5.79 D for the cis−cis, cis−trans, trans−(near-trans), and (near-trans)−(near-trans), respectively. Dipole moments of the cis−cis and cis−trans conformer calculated at MP2/aug-cc-pVQZ level of theory were 0.36 and 3.91 D, respectively, which are very close to those obtained with the double-ζ basis set.

Dipole moments were also calculated for the cis−cis and cis−trans monomers using the OPLS force field and values of 0.38 and 4.40 D, respectively, were obtained. Using the PBE functional in a plane wave (DFT/PW) basis set, dipole moments of magnitude 0.35 and 3.6 D are obtained for the cis−cis and cis−trans conformers, respectively. The PBE values are quite comparable to those obtained from MP2 calculations. Figure 5 shows dipole moments of dimethyl carbonate

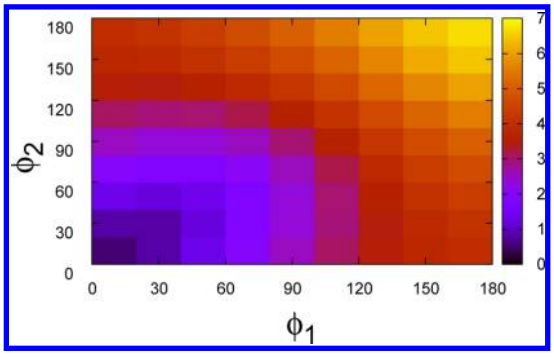


**Figure 5.** Dipole moment (in Debye) surface of dimethyl carbonate as a function of two dihedrals, $\phi_1$ and $\phi_2$. Color scale is also shown.

molecule as a function of the two dihedrals, $\phi_1$ and $\phi_2$, obtained at MP2/aug-cc-pVDZ level of theory. If two dihedrals are greater than 150°, they possess larger dipole moments, and if they are less than 30°, they possess relatively smaller values. These regions are shown in dark blue and yellow colors, respectively, in Figure 5. The high dipole moment conformers are less likely to exist in the liquid as they are unstable. Figure 2 shows the direction of dipole moment for the four stable conformers. In the case of cis−cis and near-trans−near-trans conformers, the dipole moment vector is oriented parallel to the O1−C1 bond, while in the other two conformers, the moment is oriented at a nonzero angle with respect to this vector.

*Dimers.* An examination of stable dimer configurations in the gas phase can help in a better understanding of the intermolecular structure in the liquid state. Using different combinations of cis−cis and cis−trans conformers, geometry optimization in the gas phase yielded three stable dimers, (cis−cis)−(cis−cis) (denoted as CC−CC), (cis−cis)−(cis−trans) (denoted as CC−CT), and (cis−trans)−(cis−trans) (denoted as CT−CT), as shown in Figure 6. Two hydrogen bonds are

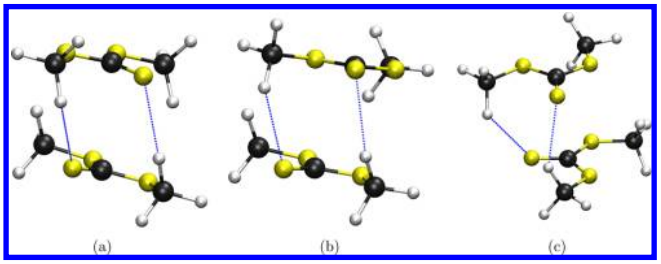


**Figure 6.** (a) (cis−cis)−(cis−cis), (b) (cis−cis)−(cis−trans), and (c) (cis−trans)−(cis−trans) dimers. Blue dotted lines are hydrogen bonds formed between atom types O and HC.

seen: one between the carbonyl oxygen of one molecule and the hydrogen (O···HC) of the other molecule and vice versa. The average h-bond length is 2.44 Å and h-bond angle is 131.7°, implying the formation of a weak hydrogen bond between the DMC molecules. Table 2 shows the relative energy

**Table 2. Binding Energy and Relative Energy (kcal/mol) of (cis−cis)−(cis−cis) (CC−CC), (cis−cis)−(cis−trans) (CC−CT), and (cis−trans)−(cis−trans) (CT−CT) Dimers Calculated at OPLS Force Field, MP2/aug-cc-pVDZ, and PBE+vdW/PW Levels of Theory**

| | CC−CC | CC−CT | CT−CT |
|---|---|---|---|
| binding energy: | | | |
| OPLS | −4.30 | −4.26 | −4.66 |
| MP2/aug-cc-pVDZ | −6.04 | −5.04 | −6.15 |
| PBE/PW | −2.72 | −5.17 | −3.59 |
| PBE+vdW/PW | −4.61 | −4.02 | −5.27 |
| relative energy:[a] | | | |
| OPLS | 0 | 2.25 | 4.06 |
| MP2/aug-cc-pVDZ | 0 | 3.83 | 5.92 |
| PBE/PW | 0 | 3.09 | 4.60 |
| PBE+vdW/PW | 0 | 3.05 | 4.27 |

[a]Values are with respect to CC−CC dimer.

and the binding energy of the three dimers calculated at MP2/aug-cc-pVDZ and PBE+vdW/PW levels of theory. Relative energy is the energy difference between a specific dimer configuration and the CC−CC one. Binding energy is the energy of stabilization of a dimer with respect to its isolated monomers. In the case of the MP2 calculation, which employed a localized basis set, these energies were corrected for the basis set superposition error (BSSE) using the counterpoise method. Among the three dimers, CC−CC is the most stable, and the CC−CT and CT−CT dimers are less stable than that by 3.83


dx.doi.org/10.1021/jp309374m | J. Phys. Chem. B 2012, 116, 14892−14902

and 5.92 kcal/mol, respectively. The binding energy of the CC−CC dimer is calculated to be −6.04 and −4.61 kcal/mol at MP2 and PBE+vdw levels of theory. Both CT−CT and CC−CC dimers have comparable binding energies and this value is greater than that of the CC−CT dimer, that is, dimers of like conformers are more stable than a dimer formed out of unlike conformers. The result is similar for data calculated at PBE +vdW/PW level. Given the fact that the CT monomer is less stable than the CC one by 3.2 kcal/mol, the relative energy difference of 5.92 kcal/mol between the CC−CC and CT−CT dimers is reasonable. Hydrogen bond lengths and angles calculated at OPLS force field, MP2/aug-cc-pVDZ and PBE +vdW/PW levels of theory are tabulated in Table 3. However,

**Table 3. Hydrogen Bond Lengths (Å) and Angles (°) Formed between (cis−cis)−(cis−cis) (CC−CC), (cis−cis)−(cis−trans) (CC−CT), and (cis−trans)−(cis−trans) (CT−CT) Dimers Calculated at OPLS Force Field, MP2/aug-cc-pVDZ, and PBE+vdW/PW Levels of Theory**

| | H-bond-I | H-bond-II |
|---|---|---|
| OPLS: | | |
| CC−CC | 2.45, 128.6 | 2.45, 128.6 |
| CC−CT | 2.45, 144.8 | 2.47, 124.5 |
| CT−CT | 2.42, 128.6 | 2.42, 128.6 |
| MP2/aug-cc-pVDZ: | | |
| CC−CC | 2.45, 129.6 | 2.45, 129.7 |
| CC−CT | 2.44, 145.9 | 2.47, 125.6 |
| CT−CT | 2.42, 129.6 | 2.42, 129.6 |
| PBE/PW: | | |
| CC−CC | 2.65, 136.6 | 2.60, 137.1 |
| CC−CT | 2.67,135.8 | 2.61, 149.6 |
| CT−CT | 2.77, 127.6 | 2.57, 137.6 |
| PBE+vdW/PW: | | |
| CC−CC | 2.50, 135.0 | 2.48, 135.7 |
| CC−CT | 2.54, 132.4 | 2.54, 151.6 |
| CT−CT | 2.56, 132.5 | 2.60, 129.6 |

the CC−CT dimer possesses one H-bond, which is more linear than the ones present in CC−CC or CT−CT dimers. For comparison, values obtained with PBE/PW (i.e., without the empirical vdW correction terms) are also tabulated in Tables 2 and 3. Hydrogen bond length and angles obtained with PBE +vdW/PW are much closer to the MP2 results than those from PBE/PW. Further, the interaction energy of two molecules both in the (cis−cis) conformation as a function of distance between them was calculated using all these methods. The same is provided in Figure S2 of Supporting Information. It further validates the usage of empirical vdW corrections to the PBE functional in our simulations.

**Liquid Structure: Molecular Dynamics.** *Pair Correlation Functions.* Figure 7 shows the intermolecular pair correlation function (PCF) between different atoms of DMC. Figure 6 shows the PCF between carbonyl carbon atoms belonging to different molecules. While the first peak is present at around 6 Å, a clear shoulder is also visible at around 4.1−4.25 Å in the functions obtained from both CPMD and FFMD. We shall examine the origin of these two features later. Compared to the FFMD liquid, molecules in the CPMD liquid are marginally closer to each other, as seen in the shift of the first peak to lower distances. At the position of the first minimum in the PCF, the coordination numbers obtained from CPMD and FFMD simulations are 14.3 (at 7.85 Å) and 12.7 (at 7.5 Å), respectively. The $g(r)$ between atom types CT−CT and OS−OS are shown in Figure 7b,c. Peak positions and widths are comparable in the two cases, CPMD and FFMD. The first maximum is marginally less intense and more broadened in CPMD compared to that in FFMD. The position of the first minimum is shifted to shorter distances.

Figure 7d shows the $g(r)$ between atom types CT and OS. It exhibits two peaks within a distance of 6 Å which are separated by less than 2 Å. These two peaks are due to the two OS type oxygen atoms present within a single molecule. The $g(r)$ between atom types O and HC is shown in Figure 7c. Significant differences are observed between the CPMD and FFMD results. In CPMD, the feature begins at 1.77 Å compared to a value of 2.05 Å obtained from the FFMD simulations. The shift in the peak to lower distances within CPMD signifies a stronger binding between hydrogen atoms of the methyl and the carbonyl oxygens (C−H···O hydrogen bonding). The first peak (at 2.85 Å) is less intense and broadened in CPMD compared to FFMD simulations. The first minimum of the CPMD PCF is at 3.15 Å and the corresponding coordination number is 2.85. Such large H-bond distances indicate that the hydrogen bond can be characterized as a weak one. We present a discussion on the conformational dependence of the O-HC g(r) later. The pair correlation function between atom types CT and O is shown in Figure 7f. The first peak (at 3.40 Å) is less intense and its position is shifted to left compared with that of FFMD, a behavior which is similar to that observed in other $g(r)$s.

The intramolecular $g(r)$ between atom types CT and OS calculated from CPMD and FFMD simulations is shown in Figure 8. The intense peak at around 3.5 Å is due to molecules in the cis−cis conformation and that, around 2.6 Å, is due to the cis−trans conformer. The ratio of area under these two features is the ratio of the population of cis−cis to cis−trans conformers. These values are 94.5:5.5 and 97.2:2.8 in FFMD and CPMD simulations, respectively.

*Dihedral Distributions and Clustering.* Figure 9 shows the probability distribution of dihedral angles for dimethyl carbonate in which both the dihedrals, C2−O2−C1−O1 and C3−O3−C1−O1 contribute. The ratio of cis−cis to cis−trans from CPMD is estimated to be 97.9:2.1, which is close to the experimental value. Two different ratios have been reported in the literature. Katon and Cohen have reported the ratio to be 99:1, whereas Chia et al. reported it to be 98:2.[12,34] However, the ratio obtained in CPMD is larger than the estimate from FFMD simulations (93.6% in favor of cis−cis). The difference between the results obtained from CPMD and FFMD is unlikely to be of any significance due to the short trajectory length of the former. The duration of the CPMD simulation is much shorter than the time scales required for conformational transitions. The latter can be estimated from barrier heights to be in the order of nanoseconds. It is beyond the scope of this manuscript to investigate the difference (if any) between the conformer populations, due to the prohibitive cost of the CPMD simulations.

The concentration of cis−trans conformers is dilute. However, the dipole moment of the cis−trans conformer is higher than that of the cis−cis conformer. Thus, it is possible that they could cluster together within the sea of cis−cis molecules. To examine this possibility, a large system containing 2532 molecules (27 times the smaller system) was simulated using FFMD. This system was equilibrated for 2 ns, and subsequently, a 8 ns trajectory was generated for analysis.

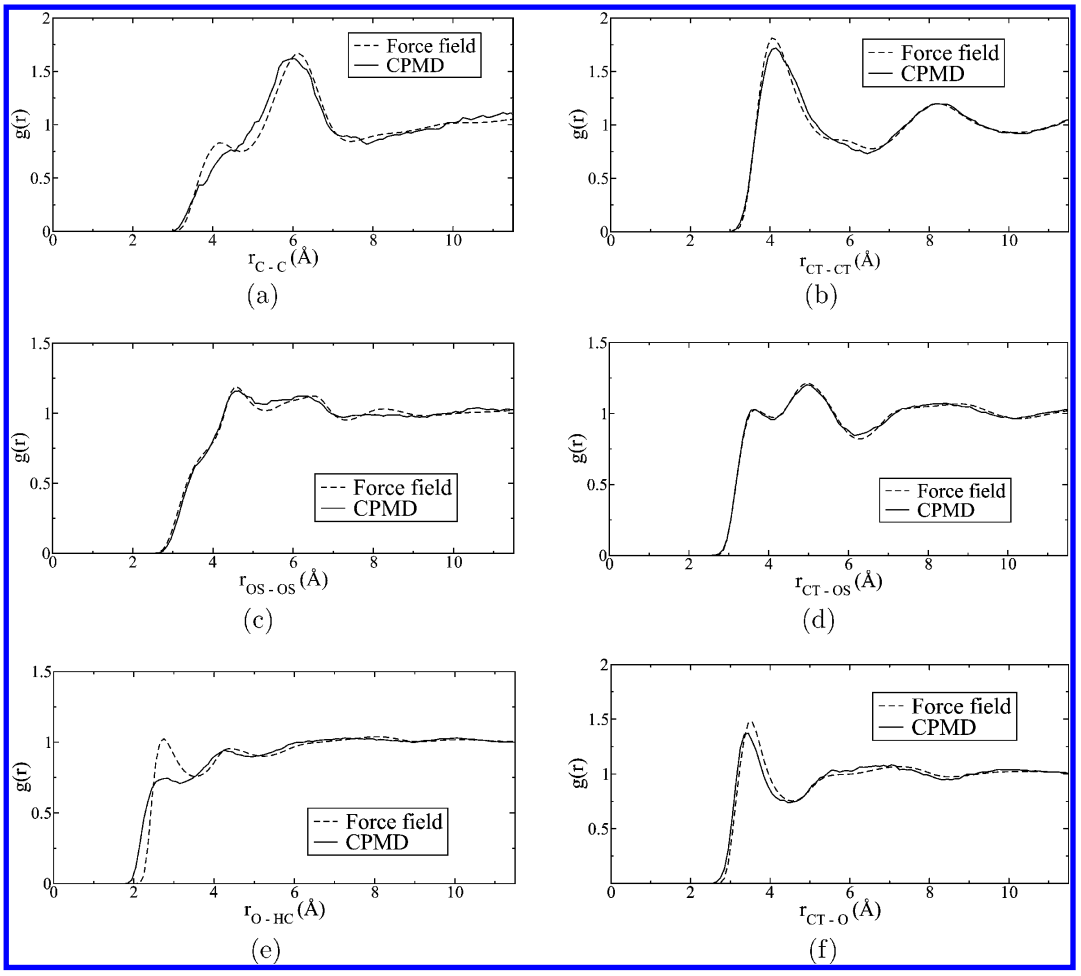


**Figure 7.** Intermolecular pair correlation functions between different pairs of atoms in liquid DMC.

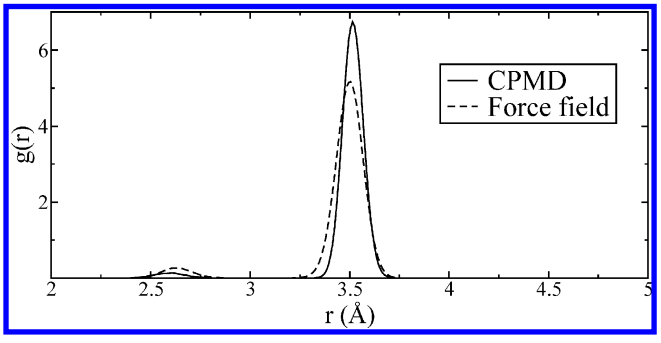


**Figure 8.** Intramolecular pair correlation function between atom types CT and OS. A bin width of 0.01 Å is used.

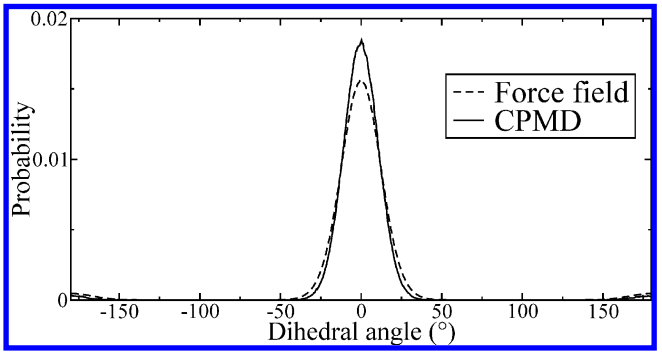


**Figure 9.** Probability distribution of dihedral angles, C2−O2−C1−O1 or C3−O3−C1−O1.

The clustering analyses was conducted as follows: If the distance between any two atoms of different CT−CT conformers is less than 3 Å, then it is considered as a cluster of size 2, and if one more molecule follows the same criteria with any of the above, then such a cluster is considered to be of size 3 and so on. During the cluster calculation, we verified that each CT−CT conformer belongs to a unique cluster. Figure 10 shows the percentage of cis−trans molecules present in clusters of different sizes. Half of the cis−trans molecules are clustered (i.e., they exist in dimers or higher oligomers) and the remaining molecules are isolated, that is, they are surrounded purely by cis−cis conformers. A snapshot of these clusters is shown in Figure 11. The observation of clustering of molecules of cis−trans conformation is consistent with the binding energy of gas phase dimers discussed in Table 2. It was seen earlier that dimers of like conformation are more stable than the one where the molecules are in different conformations. Naturally, this preference for dimerization of like conformers will lead to the formation of cis−trans clusters in the liquid phase. The clusters cannot grow to large sizes due to entropic effects.

To summarize, relative to FFMD simulations, the CPMD simulation predicts marginally closer intermolecular contacts. In particular, the formation of a weak intermolecular hydrogen bond between the carbonyl oxygen and the methyl hydrogen is observed in CPMD simulations. Clustering of cis−trans


dx.doi.org/10.1021/jp309374m | J. Phys. Chem. B 2012, 116, 14892−14902

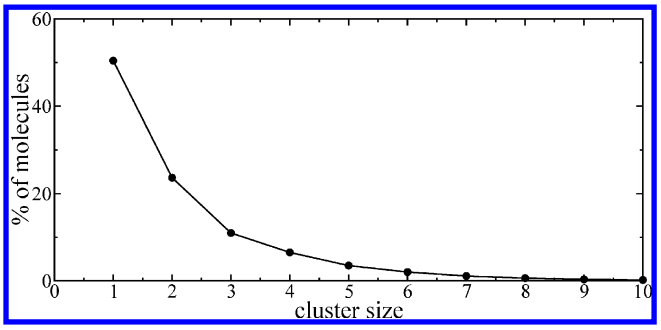


**Figure 10.** Probability distribution of the size of cluster consisting of cis−trans conformers in liquid DMC.

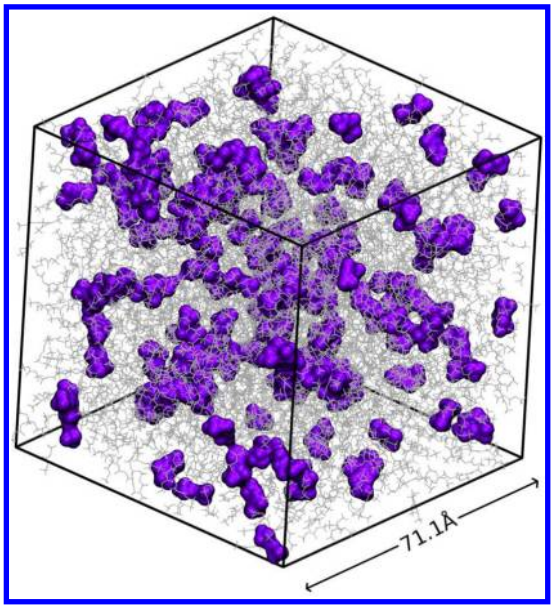


**Figure 11.** Snapshot of liquid dimethyl carbonate showing clustered cis−trans molecules along with cis−cis molecules. cis−trans and cis−cis molecules are colored in violet and gray, respectively.

molecules is observed in simulations of a large system studied using FFMD.

**Spatial Distribution Functions.** Spatial distribution functions (SDF) show the density distribution of atoms in three-dimensional space. Figure 12 shows SDF maps around the carbonyl carbon and the carbonyl oxygen in two orientations. In one of them, the carbonyl vector is perpendicular to the plane of the paper and is directed toward the reader and in the other, it is parallel to the plane of the paper and is directed upward. It is to be noted that, in this calculation, we assume the central molecule to be in cis−cis conformation. Because the percentage of other conformers is much smaller, the results are unlikely to be much affected by this assumption.

An examination of the isosurfaces of spatial distribution functions reveals the origin of the various features observed in the pair correlation functions. Molecules proximal to the methyl group are responsible for the intense peak at around 6 Å in the C−C $g(r)$ shown in Figure 7a. The shoulder at 4 Å in the same $g(r)$ is due to molecules lying in a plane parallel to the equatorial plane of the molecule. In CPMD, the distribution of molecules around the center is less ordered compared to that in FFMD as seen in Figure 12a−d. This is reflected in the C−C $g(r)$, which exhibits just a shoulder at around 4 Å distance in

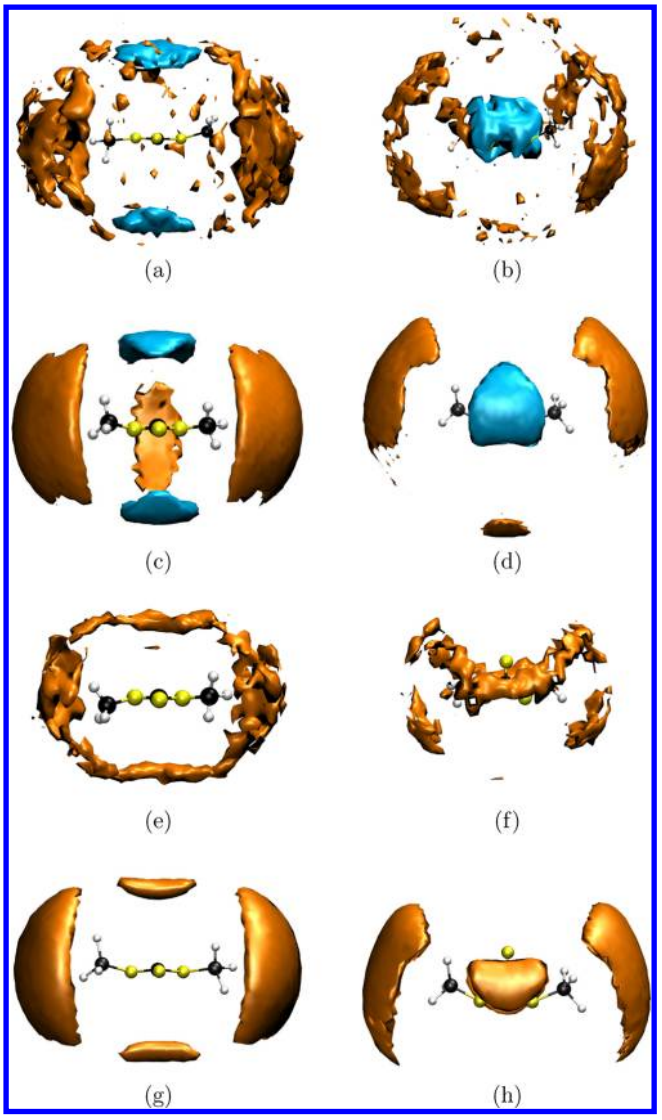


**Figure 12.** Spatial distribution functions of carbonyl carbon (a−d) and carbonyl oxygen atoms (e−h) around the center of mass of dimethyl carbonate are shown at an isosurface value of 0.0165 $Å^{-3}$. (a), (b), (e), and (f) are obtained from the CPMD run, while (c), (d), (g), and (h) are calculated from the force field based simulation. In each simulation, two views, one in which the carbonyl group is pointing toward the reader and in another, it is in the plane of the paper and pointing upward are shown. Color code: C, black; O, yellow; H, gray.

CPMD compared to the intense peak at the same distance seen in FFMD simulations (Figure 7a).

The SDF between carbonyl oxygen around the dimethyl carbonate molecule is shown in Figure 12c−h. Because of electrostatic attraction between the carbonyl oxygen and hydrogen atoms, the former are likely to be surrounded by the methyl groups. Similar to the SDF between carbon and the geometric center of DMC molecule, it too shows more ordered structure in the first coordinations shell in FFMD compared to CPMD.

To find the distance dependence of orientational preferences of dimethyl carbonate molecules around a reference molecule, the angle between two carbonyl vectors of two adjacent DMC molecules is calculated. Figure 13a shows the probability distribution of this angle between neighbors which are located within a certain cutoff distance. At the first coordination


dx.doi.org/10.1021/jp309374m | J. Phys. Chem. B 2012, 116, 14892−14902

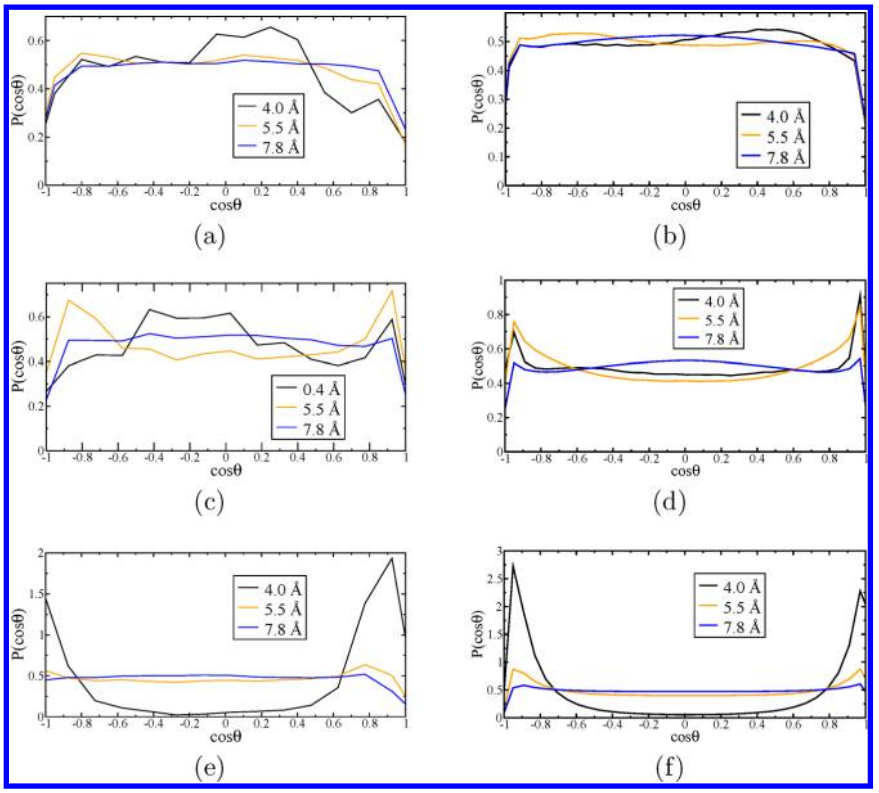


**Figure 13.** Probability distribution of angle between intermolecular (a, b): C−O vectors, (c, d) CT−CT vectors, and (e, f) normal vectors to the plane of dimethyl carbonate molecules, obtained with both density functional theory (left) and force field (right) based molecular dynamics simulations. Marked values in legends are distances between center of mass of neighboring molecules.

minimum (7.8 Å), all orientations are possible as shown in Figure 13a. At shorter distances, the distribution reveals a marginal orientational preference, which is absent in FFMD simulations. Further, the angle between two CT−CT vectors and also that between normals to the plane of adjacent DMC molecules are calculated. The distribution of these angles are shown in Figure 13c−f. The distribution between normal vectors for molecules lying very close to each other show preference toward parallel or antiparallel alignment of planes with almost no preference for perpendicular alignment. One can conclude that close lying DMC molecules are oriented parallel or antiparallel to each other and with increasing distance, all orientations become equally probable. Our analysis confirms the recent X-ray scattering and MD simulation data of Caminiti et al.[19] The CPMD data show a small preference for close lying molecules to lie with their CT−CT vectors (or C−O vectors) perpendicular to each other.

*Dipole Analysis.* Maximally localized Wannier functions have been employed successfully in numerous applications to calculate effective Born charges, the nature of chemical bonding, bond ionicity, electric polarization, and dipole moments.[30,37−39] We adopt the same procedure to obtain the molecular dipole moments here. When the position of Wannier centers is used for configurations of the liquid, the dipole moment of individual molecules in the liquid state were calculated using eq 1.

Figure 14 shows the distribution of such molecular dipole moments. Two features, an intense peak centered at around 1.0 D and another, beyond 4.0 D, are observed. The distribution obtained from the force field is shifted to slightly lower values relative to that from CPMD simulations. To find out whether this large dipole moment is due to cis−trans conformers or

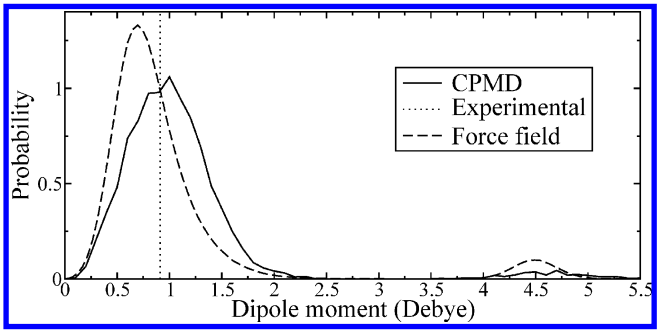


**Figure 14.** Probability distribution of molecular dipole moment in liquid dimethyl carbonate. The experimental value (0.91 D) is shown as a dotted line.[14].

(near-cis)−(near-trans) conformers, two dihedral angles of each DMC molecule are calculated. If the magnitude of two dihedrals is greater than 100° or less than −100°, they are considered as (near-cis)−(near-trans) or trans−(near-trans) conformers. This value averaged over the entire trajectory shows that only an insignificant number (0.1%) of molecules are present in that conformational state in the liquid at room temperature. Thus, the peak in the distribution beyond 4.0 D is due to cis−trans conformers alone. The cis−cis (cis−trans) conformer possesses a mean dipole moment of 1.0 D (4.5 D) in the liquid state, which is much higher than its value of 0.35 D (3.6 D) in gas phase. This indicates considerable polarization in the condensed phase. The mean dipole moments of these distributions are 1.01 and 1.05 D obtained using force field and CPMD, respectively. These are comparable to the value determined using dielectric measurements, which is 0.91 D.[14]


dx.doi.org/10.1021/jp309374m | J. Phys. Chem. B 2012, 116, 14892−14902

**Conformational Dependence of O−HC $g(r)$.** As discussed earlier, the dipole moment of the cis−trans conformer is nearly five times larger than the cis−cis one. It was also noticed that such cis−trans molecules could be clustered in the solvent. Does the higher dipole moment of this conformer lead to differences in the intermolecular structure in its neighborhood? To probe this matter further, we calculated the atom−atom pair correlation functions for a central molecule being either in the cis−cis or in the cis−trans conformation. While all other $g(r)$s for these two categories matched, that between O and HC showed significant influence of the conformation of the central molecule. Thus, we exhibit them in Figure 15. Despite the existence of quantitative

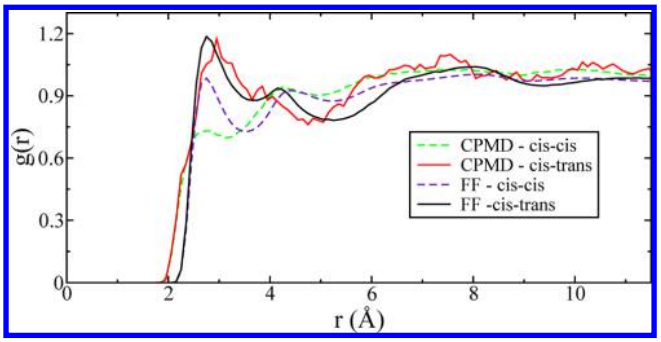


**Figure 15.** Intermolecular pair correlation functions between atom types O and HC obtained from both force field based molecular dynamics (FF) and Car−Parrinello molecular dynamics (CPMD) simulations. The legend also displays the conformational state of the central molecule.

differences between the PCFs obtained from force field or CPMD, a common trend is observed; the O−HC PCF for the case of the oxygen atom belonging to a cis−trans molecule shows a much taller first peak than around a cis−cis one. This observation tallies with the H-bond distances shown in Table 3. Although the concentration of cis−trans conformers in the liquid is very small, molecular clustering and the stronger hydrogen bonding may likely play a role in the behavior of DMC as a chemical reaction medium.

**Vibrational Spectrum.** To our knowledge, the experimental IR or Raman spectrum of deuterated liquid DMC has not been reported. Thus, we compare our results against estimates obtained on the deuterated liquid from experimental data through mass scaling.

To assign peaks in the calculated power spectrum or vibrational density of states (VDOS), the contribution of each atom to the total VDOS is calculated. Figure 16 shows the VDOS of a cis−cis monomer in gas and liquid phases and contribution from different atoms to it. Quantum effects are included in a semiclassical fashion through a factor, $\omega\beta\hbar\omega$, derived within the harmonic limit. A Hessian analysis was carried out on the gas phase cis−cis monomer to obtain its vibrational modes to aid in the assignment of modes in the liquid state. Further, CPMD trajectories at 300 K were also generated for the cis−cis and cis−trans monomers in the gas phase in order to identify if any spectral features can be assigned to a specific conformation. Peak positions found in the liquid and for the gas-phase monomer and the corresponding mode assignments are summarized in Table 4.

Peaks centered at 2108 and 2231 $cm^{-1}$ are assigned to the C−D bond stretching of the methyl group. The same peak is

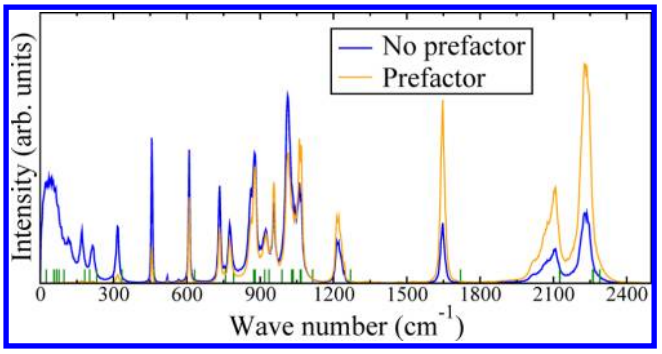


**Figure 16.** Power spectrum of deuterated liquid dimethyl carbonate in the range 0 to 2500 $cm^{-1}$. The spectrum multiplied by a prefactor, $\omega\beta\hbar\omega$, is also shown (orange). Spectrum for the cis−cis conformer in gas-phase obtained from a Hessian calculation is shown in as sticks (green).

**Table 4. Vibrational Density of States of Liquid- and Gas-Phase Monomers along with Mode Assignments[a]**

| | wave number ($cm^{-1}$) | | |
|---|---|---|---|
| Sl No. | monomer | liquid | assignment |
| 1 | 2126−2289 | 1950−2300 | $\nu CD_3$ |
| 2 | 1720 | 1647 | $\nu$(C═O) |
| 3 | 1269 | 1213, 1221 | $\nu_{as}$ OCO |
| 4 | 1114 | 1060 | $\nu_s$OCO |
| 5 | 1028−1067 | 1012 | $\delta_{ip}CD_3$ |
| 6 | 989 | | $\delta_{ip}$OCO and $CD_2$ rocking |
| 7 | 936 | | $\delta_{ip}CO_3$ and $\delta_{ip}$ OCD |
| 8 | 918 | 879 | $\nu CD_3$−O |
| 9 | 873−879 | 864 | $CD_3$ rocking |
| 10 | 791 | 775 | $\delta_{ip}$DCO |
| 11 | 758 | 734 | $\delta_{oop}CO_3$ |
| 12 | 631 | 609 | $OCO_2$ rocking |
| 13 | 465 | 456 | $\delta$OCO |

[a]Frequencies are not scaled.

expected to appear at 2740 $cm^{-1}$ in the protiated liquid (taking into account the reduced mass of the oscillator) compared to the experimental value of 3000 $cm^{-1}$. The difference is in part due to the inadequacy of the exchange-correlation functional used that has been documented earlier.[40,41] Another reason could be the artificial drag experienced by the electron in a CPMD simulation.[42,43] The C═O stretch modes is at 1647 $cm^{-1}$ in the liquid, whereas in the monomer, it appears at 1720 $cm^{-1}$. In the region 1500−1700 $cm^{-1}$, oxygen and carbon of the carbonyl group contribute to the total VDOS, while other atoms contribute much less, as seen from Figure 17. Asymmetric stretching of the OCO group shows peaks at 1213 and 1221 $cm^{-1}$, whereas symmetric stretching is observed at 1060 $cm^{-1}$. The experimental values of these modes show peaks at 1279 and 1120 $cm^{-1}$, respectively. Peak centered at 1012 $cm^{-1}$ is due to bending of the $CD_3$ group. The VDOS of carbon and hydrogen atoms are clearly contributing more to the total VDOS in this region as seen from Figure 17. A peak at 879 $cm^{-1}$ is assigned to the stretching of $CD_3$−O group. The rocking motion of $CD_3$ group is observed at 864 $cm^{-1}$. From Figure 17, we notice that this peak also has contribution from OS type oxygens. Bending of HCO group contributes to the peak at 775 $cm^{-1}$. The feature at 734 $cm^{-1}$ can be assigned to out-of-plane motion of $CO_3$ group. Carbonyl oxygen and carbonyl carbon contribute more to this peak than other


dx.doi.org/10.1021/jp309374m | J. Phys. Chem. B 2012, 116, 14892−14902

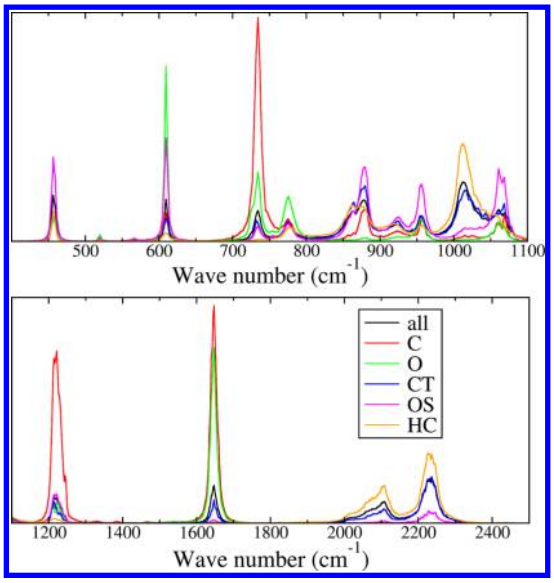


**Figure 17.** Power spectrum of deuterated liquid dimethyl carbonate in the range 400−1100 $cm^{-1}$ (top) and 1100−2500 $cm^{-1}$ (bottom) compared with its atomically decomposed vibrational density of states. *y*-Axis in bottom figure is scaled for clarity. Label scheme is same in both the panels.

oxygen atoms as clearly seen in Figure 17. A peak centered at 609 $cm^{-1}$ is assigned to the rocking motion of $OCO_2$ group. In this mode, all oxygens contribute more than any other atoms to the total VDOS. Significantly, the spectrum of the cis−trans monomer in the gas phase exhibits a feature at around 525 $cm^{-1}$, which could be assigned to the same mode. Thus, the exact location of the $OCO_2$ rocking mode can be used to distinguish between the two conformational states of DMC. The peak at 456 $cm^{-1}$ is assigned to in-plane bending of the OCO group. Taking into account the substitution of deuterium for hydrogen, all calculated peak positions are more or less red-shifted compared to experimental values.

## 4. DISCUSSION AND CONCLUSIONS

We have carried out extensive MD simulations of an environmentally benign solvent and chemical reaction medium, dimethyl carbonate, based both on quantum density functional theory as well as on an empirical force field. The liquid modeled with CPMD is predominantly constituted by molecules in the cis−cis conformation, whereas only about 2% (6% in force field based simulations) of molecules are present in the cis−trans conformation, under ambient conditions. The mean value of the molecular dipole moment calculated from our simulations agrees well with results from dielectric measurements.[14]

The DFT-based Car−Parrinello MD simulations were augmented with empirical van der Waals corrections. They predict slightly shorter intermolecular contacts than those from force field simulations, in particular for the carbonyl oxygen−methyl hydrogen distance. The dipole moment of molecules in the cis−trans conformation is around 4.5D, while the value for those in the cis−cis conformation is around 1.0D. This wide disparity in the dipole moment magnitudes can lead to heterogeneity in the liquid, although the concentration of molecules in the cis−trans conformation is dilute. Indeed, we have observed clustering of cis−trans molecules that arises from the higher binding energy (i.e., more stable) of dimers of like conformers than that of unlike conformers.

In the liquid, close neighbors of DMC lie with their molecular planes parallel to each other. However, the dipole vectors of neighboring molecules do not show a preference for any specific orientation. Neighbors tend to form weak C−H···O hydrogen bond with a central molecule and the tendency increases when the central molecule is a cis−trans conformer. Vibrational mode assignments obtained from our condensed phase CPMD simulations are in excellent agreement with experiments.

Our work has demonstrated the salient features of intermolecular structure and dynamics of this environmentally benign solvent. Simulations to discern the solvent's role in the conduct of specific chemical reactions can now be undertaken.

## ■ ASSOCIATED CONTENT

### Ⓢ Supporting Information

Comparison of the pair correlation function between atom types O and HC. This material is available free of charge via the Internet at http://pubs.acs.org.

## ■ AUTHOR INFORMATION

### Notes

The authors declare no competing financial interest.

## ■ ACKNOWLEDGMENTS

We thank the Department of Science and Technology for support. We also thank the Centre for Development of Advanced Computing (C-DAC), Bangalore and the CSIR Centre for Mathematical Modelling and Computer Simulation (CSIR C-MMACS), Bangalore, where parts of these calculations were carried out. S.K.R is grateful to CSIR, India, for a senior research fellowship.

## ■ REFERENCES

(1) Anastas, T. P.; Warner, J. C. *Green Chemistry Theory and Practice*; Oxford University Press: New York, 1998.
(2) Tundo, P.; Selva, M. *Acc. Chem. Res.* **2002**, *35*, 706.
(3) Righi, G.; Bovicelli, P.; Barontini, M.; Tirotta, I. *Green Chem.* **2012**, *14*, 495.
(4) Ono, Y. *Pure Appl. Chem.* **1996**, *68*, 367.
(5) Rounce, P.; Tsolakis, A.; Leung, P.; York, A. P. E. *Energy Fuels* **2010**, *24*, 4812.
(6) Lu, X. C.; Yang, J. G.; Zhang, W. G.; Huang, Z. *Energy Fuels* **2005**, *19*, 1879.
(7) Gaylor, P. J. Modified Fuel. U.S. Patent 2,331,386, Standard Oil Development Co., 1943.
(8) (a) Yoshio, O. *Catal. Today* **1997**, *35*, 15. (b) Bernini, R.; Mincione, E.; Barontini, M.; Crisante, F.; Fabrizi, G. *Tetrahedron* **2007**, *63*, 6895.
(9) Schäffner, B.; Schäffner, F.; Verevkin, S. P.; Borner, A. *Chem. Rev.* **2010**, *110*, 4554.
(10) Inamoto, K.; Hasegawa, C.; Hiroya, K.; Kondo, Y.; Osako, T.; Uozumi, Y.; Doi, T. *Chem. Commun.* **2012**, *48*, 2912.
(11) Inamoto, K.; Campbell, L. D.; Doi, T.; Koide, K. *Tetrahedron Lett.* **2012**, *53*, 3147.
(12) Katon, J. E.; Cohen, M. D. *Can. J. Chem.* **1974**, *52*, 1994. Katon, J. E.; Cohen, M. D. *Can. J. Chem.* **1975**, *53*, 1378.
(13) Bohets, H.; van der Veken, B. J. *Phys. Chem. Chem. Phys.* **1999**, *1*, 1817.
(14) Thiebaut, J.; Rivail, J.; Greffe, J. *J. Chem. Soc., Faraday Trans. 2* **1976**, *72*, 2024.
(15) Mijlhoff. *J. Mol. Struct.* **1977**, *36*, 334.
(16) Okada, O. *Mol. Phys.* **1998**, *93*, 153.

(17) Soetens, J. *J. Mol. Liq.* **2001**, *92*, 201.
(18) Jorgensen, W. L; Maxwell, D. S.; Tirado-Rives, J. *J. Am. Chem. Soc.* **1996**, *118*, 11225. Watkins, E. K.; Jorgensen, W. L. *J. Phys. Chem. A* **2001**, *105*, 4118.
(19) Gontrani, L.; Russina, O.; Marincola, F. C.; Caminiti, R. *J. Chem. Phys.* **2009**, *131*, 244503.
(20) Frisch, M. J.; et al. *Gaussian 09*, Revision B. 01; Gaussian Inc: Wallingford, CT, 2010.
(21) Plimpton, S. *J. Comput. Phys.* **1995**, *117*, 1 http://lammps.sandia.gov.
(22) Hutter, J.; Ballone, J. P.; Bernasconi, M.; Focher, P.; Fois, E.; Goedecker, S.; Marx, D.; Parrinello, M.; Tuckerman, M. E. *CPMD*, version 3.13.2; Max Planck Institut fuer Festkoerperforschung and IBM Zurich Research Laboratory: Stuttgart, Germany, and Zurich, 1990.
(23) Kuo, I. W.; Mundy, C. J.; McGrath, M. J; Siepmann, J. I.; VandeVondele, J.; Sprik, M.; Hutter, J.; Chen, B.; Klein, M. L.; Mohamed, F.; Krack, M.; Parrinello, M. *J. Phys. Chem. B* **2004**, *108*, 12990.
(24) Wendler, K.; Brehm, M.; Malberg, F.; Kirchner, B.; Site, L. D. *J. Chem. Theory Comput.* **2012**, *8*, 1570.
(25) Martyna, G. J.; Klein, M. L.; Tuckerman, M. *J. Chem. Phys.* **1992**, *97*, 2635.
(26) Troullier, N.; Martins, J. L. *Phys. Rev. B* **1991**, *43*, 1993.
(27) Perdew, J. P.; Burke, K.; Emzerhof, M. *Phys. Rev. Lett.* **1996**, *77*, 3865.
(28) Williams, R. W.; Malhotra, D. *Chem. Phys.* **2006**, *327*, 54.
(29) Balasubramanian, S.; Kohlmeyer, A.; Klein, M. L. *J. Chem. Phys.* **2009**, *131*, 144506.
(30) Silvestrelli, P. L.; Bernasconi, M.; Parrinello, M. *Chem. Phys. Lett.* **1997**, *277*, 478.
(31) Jmol: An open-source Java viewer for chemical structures in 3D; http://www.jmol.org/
(32) McMahon, B.; Hanson, R. M. *J. Appl. Crystallogr.* **2008**, *41*, 811.
(33) Humphrey, W.; Dalke, A.; Schulten, K. *J. Mol. Graphics* **1996**, *14*, 33.
(34) Chia, L. H. L.; Kwan, K. J.; Huang, H. H. *Aust. J. Chem.* **1981**, *34*, 349.
(35) Labrenz, D.; Schroer, W. *J. Mol. Struct.* **1991**, *249*, 327.
(36) Bohets, H.; van der Veken, B. J. *Phys. Chem. Chem. Phys.* **1999**, *1*, 1817.
(37) Silvestrelli, P. L.; Marzari, N.; Vanderbilt, D.; Parrinello, M. *Solid State Commun.* **1998**, *7*, 107.
(38) Silvestreli, P. L.; Parrinello, M. *J. Chem. Phys.* **1999**, *111*, 3572.
(39) Silvestreli, P. L.; Parrinello, M. *Phys. Rev. Lett.* **82**, 3308.
(40) Reddy, S. K.; Kulkarni, C. H.; Balasubramanian, S. *J. Chem. Phys.* **2011**, *134*, 124511.
(41) Handgraaf, J. -W.; Meijer, E. J. *J. Chem. Phys.* **2004**, *121*, 10111.
(42) Kirchner, B.; Hutter, J. *J. Chem. Phys.* **2004**, *121*, 5133.
(43) Amira, S.; Spångberg, D.; Hermansson, K. *J. Chem. Phys.* **2006**, *124*, 104501.